

# Linearization of the Two Link Robot Arm

Tarik Tosun, MAE 345 Assignment 4

10/20/11

## Abstract

In this assignment, the dynamics of the Type 2 two-link robotics manipulator (explored in the previous assignment) were linearized about certain points. In doing this, we show the effectiveness of linearization in simplifying the analysis of complicated nonlinear dynamic systems.

## 1 Linearization of the State Space Model

### 1.1 Derivation of $F(t)$ and $G(t)$ from State Space Model

Taking the first-order linearization of the state space model, we aim to express the system in the form:

$$\dot{x}(t) \approx \mathbf{f}[\mathbf{x}_N(t), \mathbf{u}_N(t)] + \mathbf{F}(t) \Delta \mathbf{x}(t) + \mathbf{G}(t) \Delta \mathbf{u}(t)$$

Taking the first-order linearization of the state space model, we find:

$$\mathbf{F}(t) = \begin{bmatrix} 0 & 1 & 0 \\ 0 & \left( \frac{x_4 \sin(2x_3)}{\cos^2(x_3)} \right) \Big|_{eq} & \left( \frac{x_2 x_4 \sin(2x_3) + \frac{u_1}{ml^2}}{\cos^2(x_3)} \right) \Big|_{eq} \\ 0 & 0 & 0 \\ 0 & \left( \frac{-\sin(2x_3)}{2} \right) \Big|_{eq} & \left( \frac{g}{l} \sin(x_3) - x_2 \cos(2x_3) \right) \Big|_{eq} \end{bmatrix}$$
$$\mathbf{G}(t) = \begin{bmatrix} 0 & 0 \\ \left( \frac{1}{ml^2 \cos^2(x_3)} \right) \Big|_{eq} & 0 \\ 0 & 0 \\ 0 & \frac{1}{ml^2} \end{bmatrix}$$

### 1.2 Constant Conditions

We wish to determine the circumstances under which  $\mathbf{F}$  and  $\mathbf{G}$  are constant. By inspecting the matrices, we see that  $x_2$ ,  $x_3$  and,  $x_4$ , and  $u_1$  must be constant in order for  $\mathbf{F}$  and  $\mathbf{G}$  to be constant. Both  $u_2$  and  $x_1$  may vary freely.

## 2 Analysis about $\theta_{3_N} = 0^\circ, \pm 45^\circ$

We wish to analyze the system under the conditions  $\theta_{1_N} = x_{1_N} = \text{constant}$  and  $x_{2_N} = x_{4_N} = 0$ .  $\theta_{2_N} = x_{3_N}$  will take on the values  $-45^\circ, 0^\circ$ , and  $45^\circ$ .

## 2.1 Numerical Values of $\mathbf{F}$ and $\mathbf{G}$

The numerical values of  $\mathbf{F}$  and  $\mathbf{G}$  under these three conditions are:

$x_3 = -45^\circ$ :

$$\mathbf{F}(t) = \begin{bmatrix} 0 & 1 & 0 & 0 \\ 0 & 0 & 0 & 0 \\ 0 & 0 & 0 & 1 \\ 0 & 0.5 & -6.93 & 0 \end{bmatrix} \quad \mathbf{G}(t) = \begin{bmatrix} 0 & 0 \\ 1 & 0 \\ 0 & 0 \\ 0 & 0.5 \end{bmatrix}$$

$x_3 = 0$ :

$$\mathbf{F}(t) = \begin{bmatrix} 0 & 1 & 0 & 0 \\ 0 & 0 & 0 & 0 \\ 0 & 0 & 0 & 1 \\ 0 & 0 & 0 & 0 \end{bmatrix} \quad \mathbf{G}(t) = \begin{bmatrix} 0 & 0 \\ 0.5 & 0 \\ 0 & 0 \\ 0 & 0.5 \end{bmatrix}$$

$x_3 = 45$ :

$$\mathbf{F}(t) = \begin{bmatrix} 0 & 1 & 0 & 0 \\ 0 & 0 & 0 & 0 \\ 0 & 0 & 0 & 1 \\ 0 & -0.5 & 6.93 & 0 \end{bmatrix} \quad \mathbf{G}(t) = \begin{bmatrix} 0 & 0 \\ 1 & 0 \\ 0 & 0 \\ 0 & 0.5 \end{bmatrix}$$

## 2.2 Eigenvalues of $\mathbf{F}$

The Eigenvalues of  $\mathbf{F}$  under these three conditions are:

$x_3 = -45^\circ$ :  $\lambda = \pm 2.63i, 0, 0$

$x_3 = 0$ :  $\lambda = 0, 0, 0, 0$

$x_3 = 45$ :  $\lambda = \pm 2.63, 0, 0$

## 2.3 Initial Angular Rate Perturbations

We seek that values  $\Delta u_1$  and  $\Delta u_2$  that will produce initial rate perturbations  $\Delta x_2(0)$  and  $\Delta x_4(0)$  of  $0.1^\circ/\text{sec}$  under these three conditions. In order to accurately determine these values, we would need to investigate the impulse response of the system. As this was not covered in class, the following values will be used:

$x_{3_N}$	$\Delta u_1$	$\Delta u_2$
$-45^\circ$	0.1	0.2
$0^\circ$	0.2	0.2
$45^\circ$	0.1	0.2

These values were derived by dividing 0.1 by the corresponding values in the  $\mathbf{G}$  matrix for each of the three conditions so that in all cases the forcing term will be equal to 0.1. This is not equivalent to an impulse response, but at least provides some normalization of the inputs according to the  $\mathbf{G}$  matrix.

## 2.4 Step Response to $\Delta u_2$

Please note: Here I am choosing to discuss the response to  $\Delta u_2$  first, and  $\Delta u_1$  second. The system responses to step inputs have been computed and plotted for the values of  $\Delta u_2$  given above, and are shown in Figures 1, 2, and 3. In all figures, the step occurs at  $t = 1\text{sec}$ . The step responses illustrate the stability of the system about each of the three equilibrium points explored. Physically, it corresponds to the instantaneous application of a small constant upwards torque at the joint where the transverse arm meets the upright link. For  $x_{3_N} = 45^\circ$ , we see that the step input quickly drives the system unstable. This can be explained in terms of the system's eigenvalues:  $\lambda = \pm 2.63, 0, 0$ . They are all real, indicating a non-oscillatory response, and one of them is positive, indicating instability. If a system has even one positive eigenvalue, it will be asymptotically unstable- as time increases, the modes of the system governed by positive eigenvalues will grow, while those governed by negative eigenvalues will tend towards zero, causing the unstable modes to dominate.

For  $x_{3_N} = 0^\circ$ , we also see the system's response growing in an unbounded fashion, albeit more slowly than for  $x_{3_N} = 45^\circ$ . In this case, the system's eigenvalues are  $\lambda = 0, 0, 0, 0$ . This indicates that the system's dynamics are constant, and its response is exactly proportional to the input. The angular acceleration of  $\Delta \theta_2$  is constant and proportional to the constant input  $\Delta u_2$ , so we see  $\Delta x_4$  increasing linearly and  $\Delta x_3$  increasing quadratically.

The system's response for  $x_{3_N} = -45^\circ$  is quite different from that at either of the other two positions - it is stable. We see that the system's nonzero eigenvalues are  $\lambda = \pm 2.63i, 0, 0$ . They are purely imaginary, consistent with constant-amplitude oscillation (which is exactly what we see). Notice that  $\Delta x_4$  oscillates about zero, while  $\Delta x_3$  oscillates about position slightly above zero. This is point at which the constant input torque and the torque due to gravity (accounted for in the system dynamics matrix) are equal.

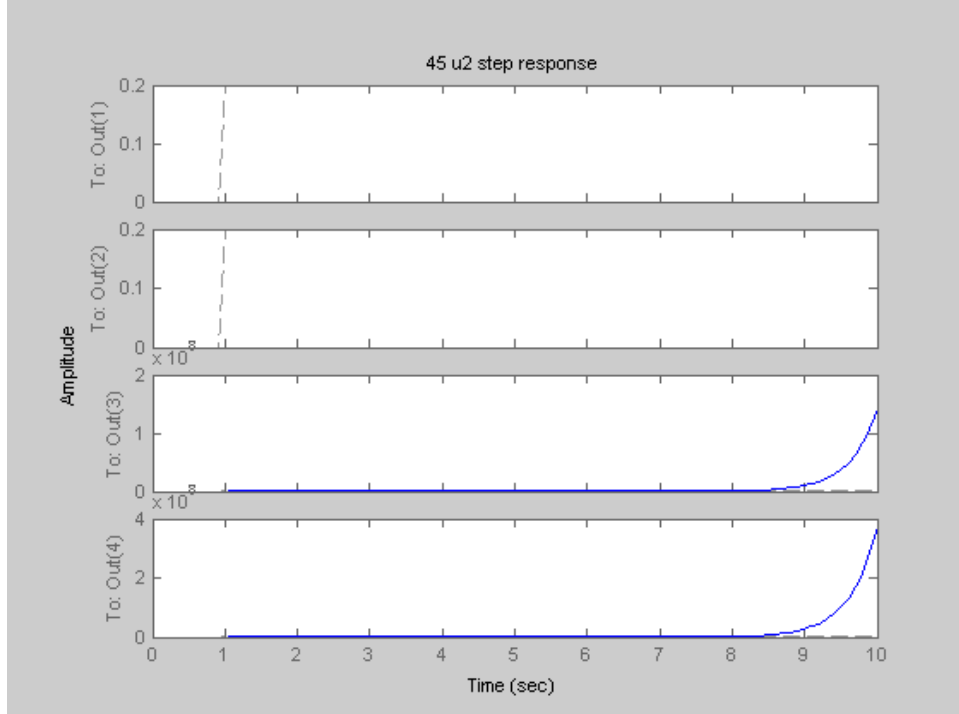


Figure 1:  $x_{3_N} = 45^\circ$  step response to  $\Delta u_2$

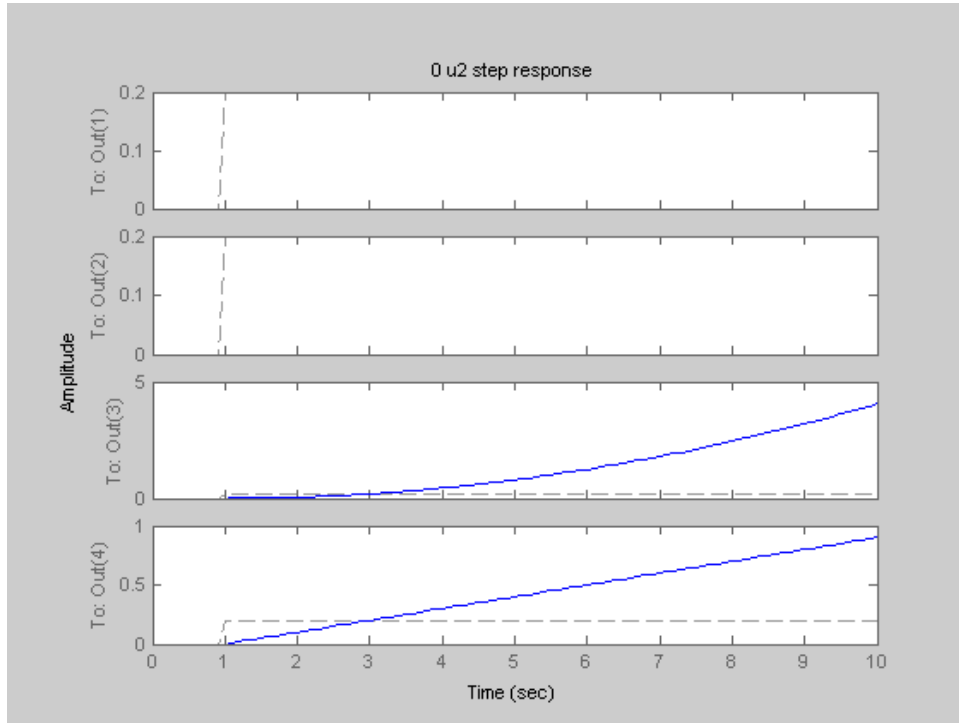


Figure 2:  $x_{3N} = 0^\circ$  step response to  $\Delta u_2$

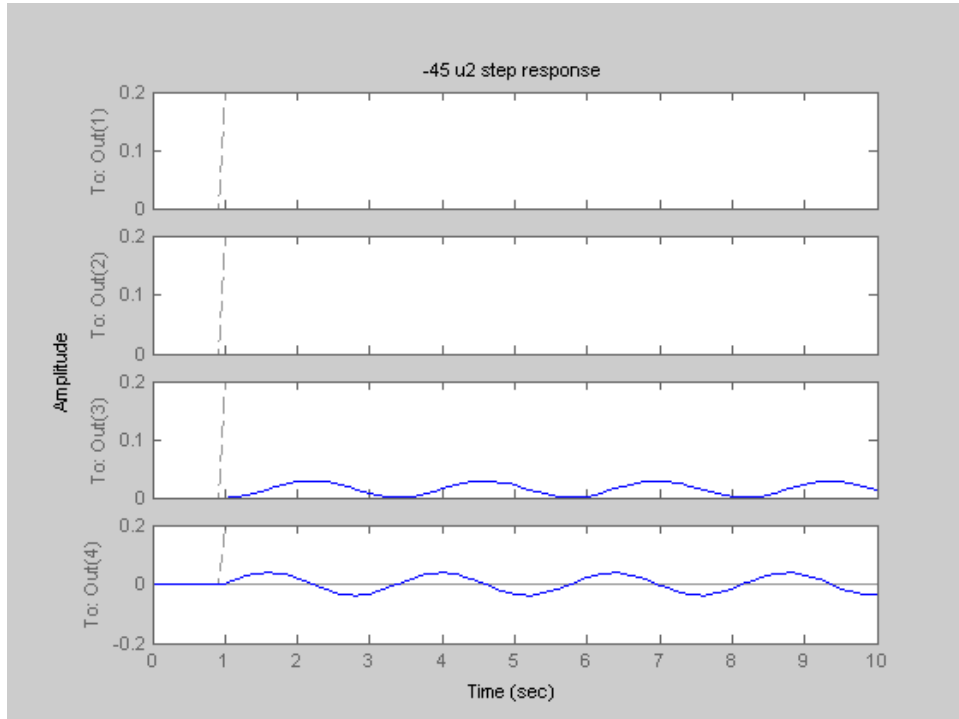


Figure 3:  $x_{3N} = -45^\circ$  step response to  $\Delta u_2$

## 2.5 Step Responses to $\Delta u_1$

The system responses to step inputs have been computed and plotted for the values of  $\Delta u_1$  given above, and are shown in Figures 4, 5, and 6. As before, the step occurs at  $t = 1 \text{ sec}$ .

The responses can again be explained in terms of the eigenvalues. Examining the responses, we see that the third and fourth eigenvalues of the dynamics matrices (which take on zero values in all three cases) correspond to modes of motion in the  $\Delta x_1$  and  $\Delta x_2$ . These states exhibit constant dynamics under all three conditions, with  $\Delta x_1$  increasing linearly and  $\Delta x_2$  increasing quadratically. However,  $\Delta x_4$  (and therefore  $\Delta x_3$ ) is coupled to  $\Delta x_2$  when  $\theta_{2_N} = x_{3_N} \neq 0^\circ$ , so under these conditions we would expect to see exponential and oscillatory responses in  $\Delta x_3$  and  $\Delta x_4$ . Inspecting the figures, that is exactly what we see. When  $x_{2_N} = 45^\circ$ , we see exponential growth in  $\Delta x_3$  and  $\Delta x_4$  due to the real positive eigenvalue that governs their behavior under these conditions. When  $x_{2_N} = -45^\circ$ , we see a purely oscillatory response in  $\Delta x_4$ , and an oscillatory but increasing response in  $\Delta x_3$ . There is motion on two time scales here. On the slow time scale, we see the 'equilibrium angle' of the transverse arm (the angle at which the gravitational and centripetal torques are equal) increase linearly with increasing angular velocity. On the fast time scale, we see oscillations about this 'equilibrium angle' due to the oscillatory mode of the first two imaginary eigenvalues. For  $x_{3_N} = 0^\circ$ , the first two states are decoupled from the second two states, so we see no response in  $\Delta x_3$  and  $\Delta x_4$ .

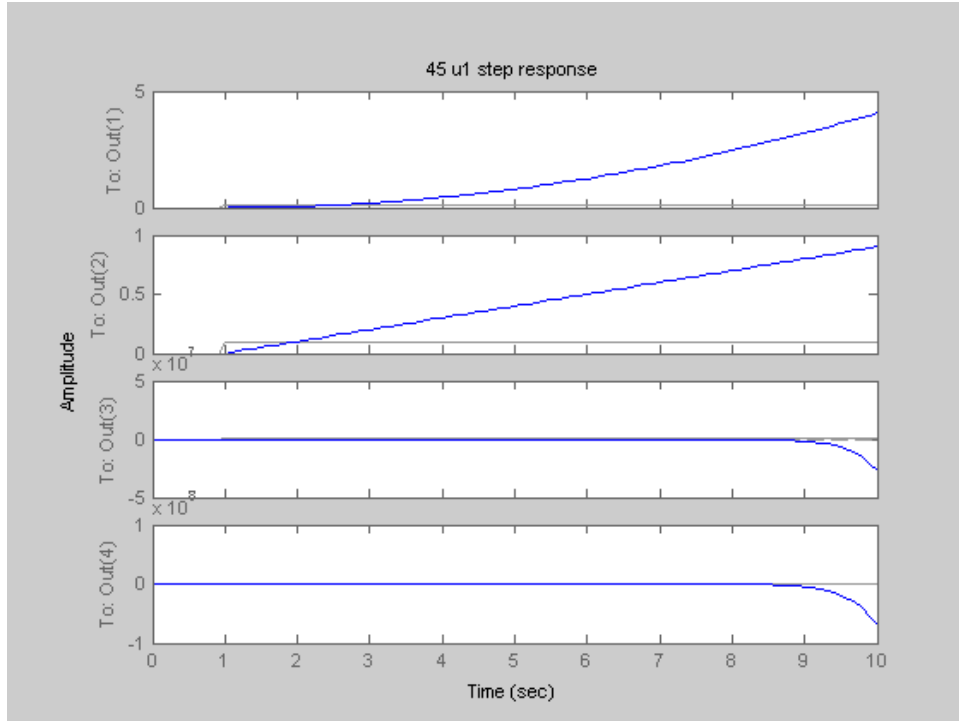


Figure 4:  $x_{3_N} = 45^\circ$  step response to  $\Delta u_1$

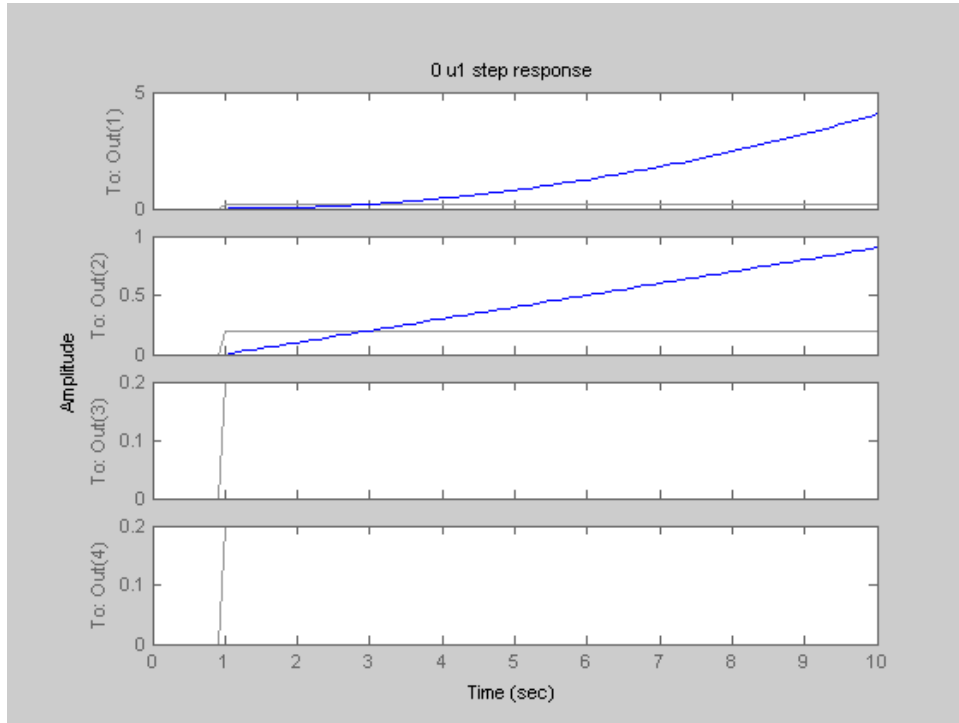


Figure 5:  $x_{3N} = 0^\circ$  step response to  $\Delta u_1$

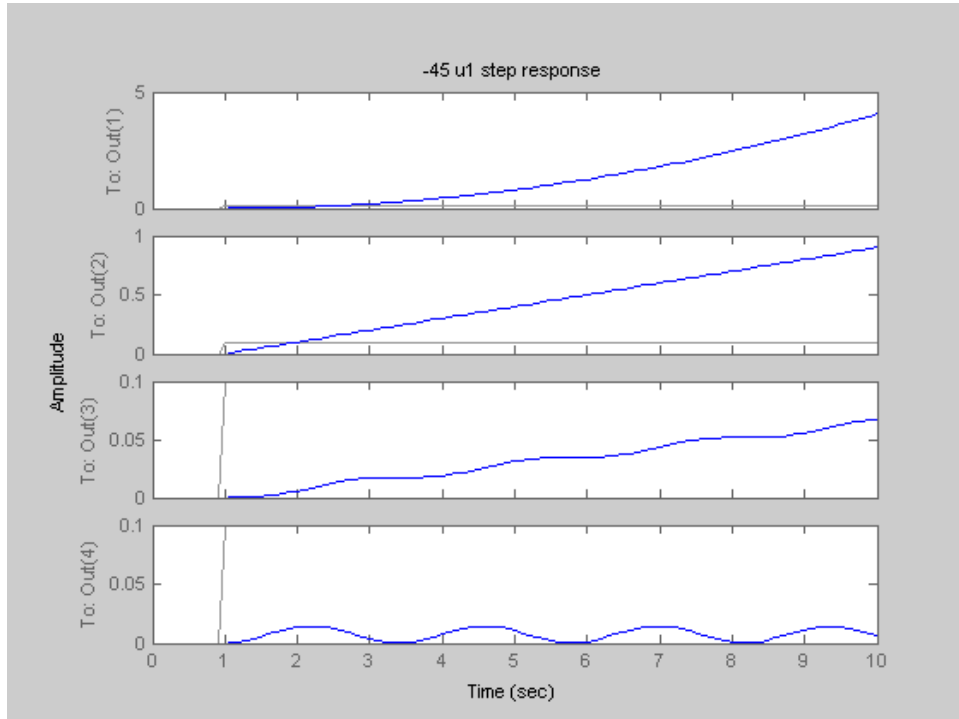


Figure 6:  $x_{3N} = -45^\circ$  step response to  $\Delta u_1$

## 2.6 Bode Plots for $\Delta u_2$ inputs

Bode plots for gain from input  $\Delta u_2$  to system states  $\Delta x_4$  and  $\Delta x_3$  have been computed for each of the three states discussed previously. Bode plots for gain from  $\Delta u_2$  to  $\Delta x_2$  and  $\Delta x_1$  were not plotted, because these gains are always zero ( $\Delta u_2$  is a torque on the transverse arm, and has no effect on the rotation of the upright link).

Bode plots for  $x_{3_N} = 45^\circ$  are shown in Figures c and 8 below. For  $\frac{\Delta x_3(j\omega)}{\Delta u_2(j\omega)}$ , we see a steady gain of about -23db for low frequencies, with gain dropping off at -40db/decade for increasing frequencies after the two poles at 2.36 rad/sec. Intuitively this makes sense, as we would expect the angular inertia of the arm to make it a natural “low-pass filter.” When we consider  $\frac{\Delta x_4(j\omega)}{\Delta u_2(j\omega)}$ , we are dealing with the derivative of  $\frac{\Delta x_3(j\omega)}{\Delta u_2(j\omega)}$ . In the frequency domain, this corresponds to multiplying the transfer function of  $\frac{\Delta x_3(j\omega)}{\Delta u_2(j\omega)}$  by  $s$ , or adding a zero at zero frequency. When we look at 8, we see that it does indeed correspond to 8 with a zero added at zero frequency.

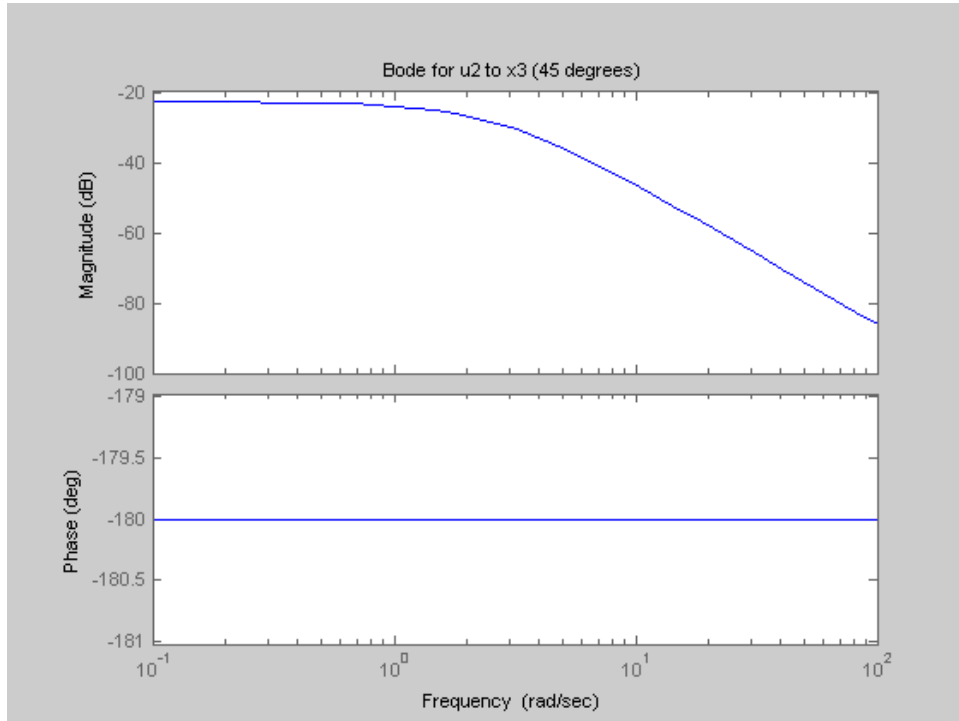


Figure 7: Bode plot for  $\frac{\Delta x_3(j\omega)}{\Delta u_2(j\omega)}$  for  $\Delta x_{3_N} = 45^\circ$

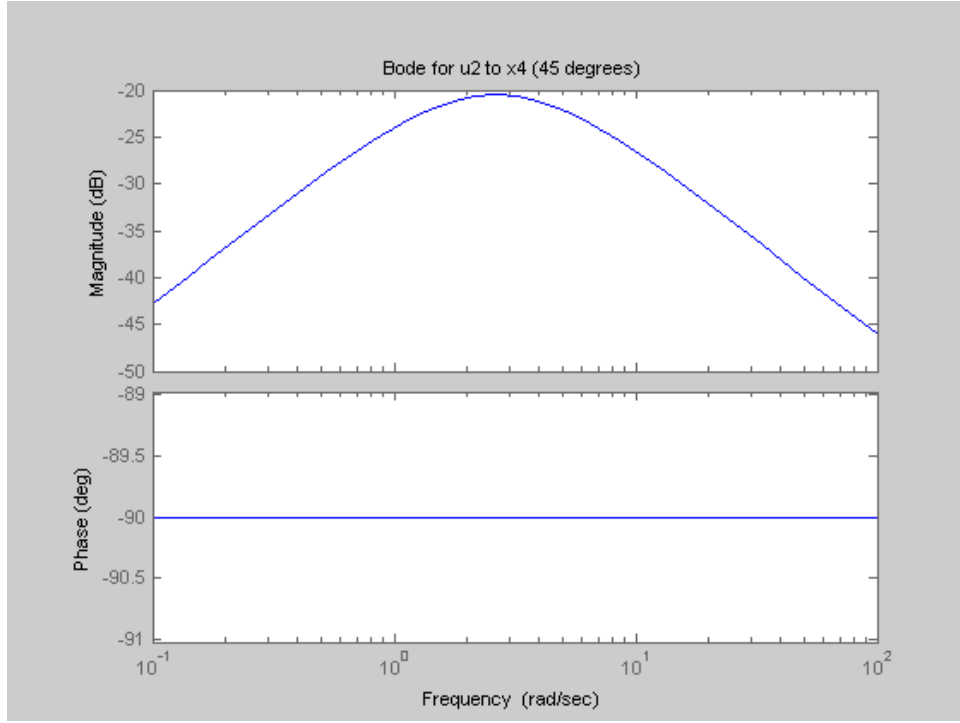


Figure 8: Bode plot for  $\frac{\Delta x_4(j\omega)}{\Delta u_2(j\omega)}$  for  $\Delta x_{3_N} = 45^\circ$

Bode plots for  $x_{3_N} = 0^\circ$  are shown in Figures 9 and 10 below. As expected, in Figure 9 we see a second-order pole at zero (corresponding to the zero eigenvalues), evidenced by the downward slope of -40db/decade. In Figure 10, we see a downward slope of only -20db/decade, due to the fact that  $\Delta x_4$  is the derivative of  $\Delta x_3$ , placing a zero at zero frequency.



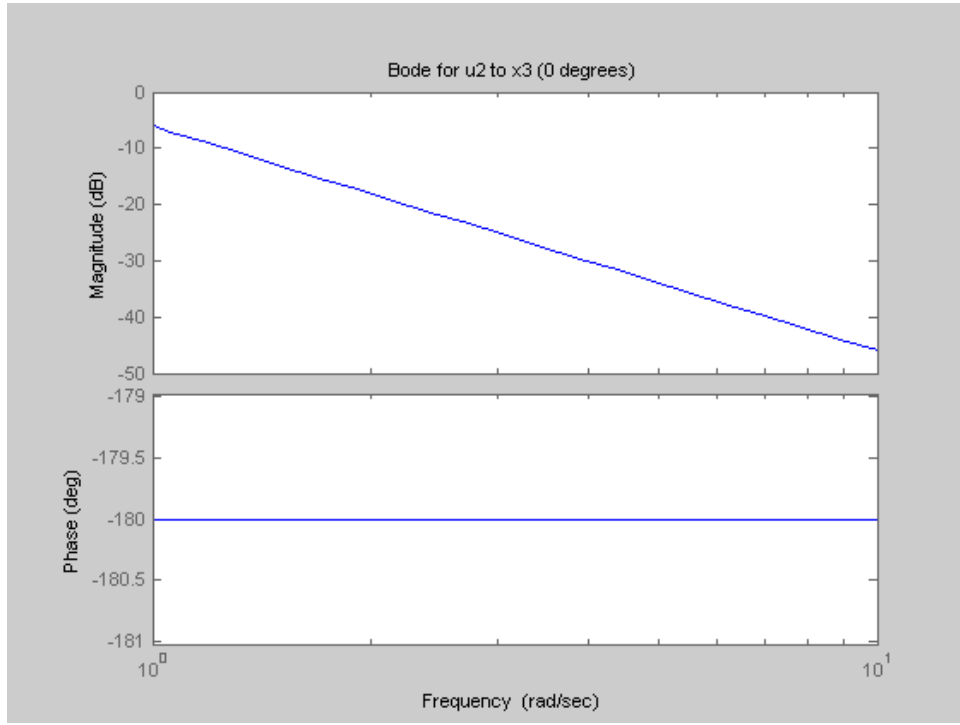


Figure 9: Bode plot for  $\frac{\Delta x_3(j\omega)}{\Delta u_2(j\omega)}$  for  $\Delta x_{3N} = 0^\circ$

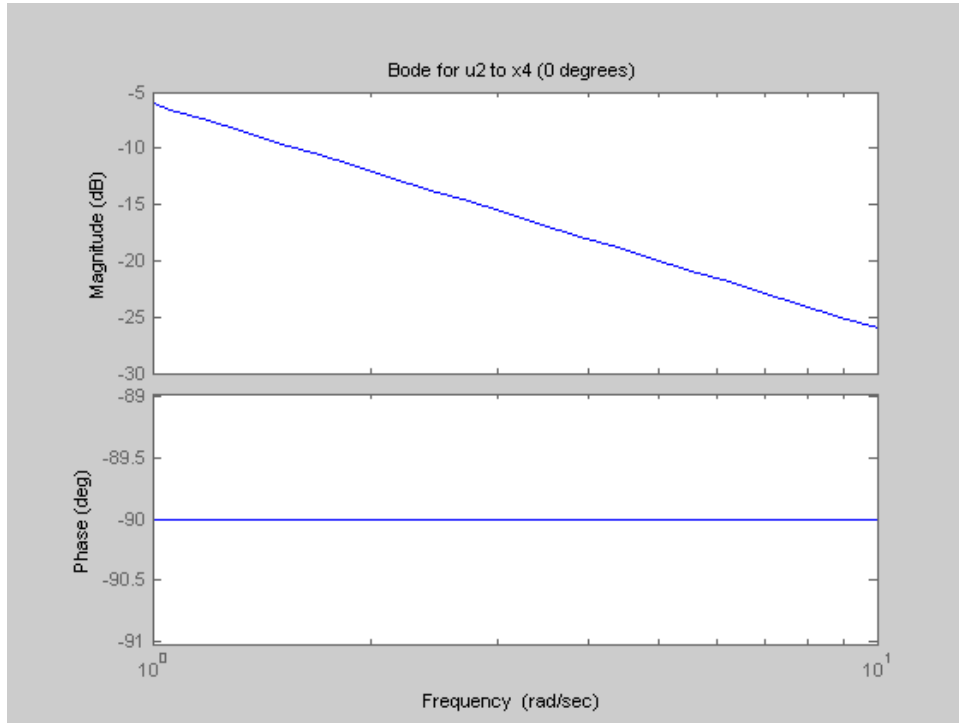


Figure 10: Bode plot for  $\frac{\Delta x_4(j\omega)}{\Delta u_2(j\omega)}$  for  $\Delta x_{3N} = 0^\circ$

Bode plots for  $x_{3N} = -45^\circ$  are shown in Figures 11 and 12 below. We see the typical response of a second-order oscillatory system here, with a clear resonant peak at 2.63. Because the system has no damping, the peak is infinite, and the phase drop is a sharp right angle. Were damping included in the model, the curves would become increasingly smooth with greater damping.

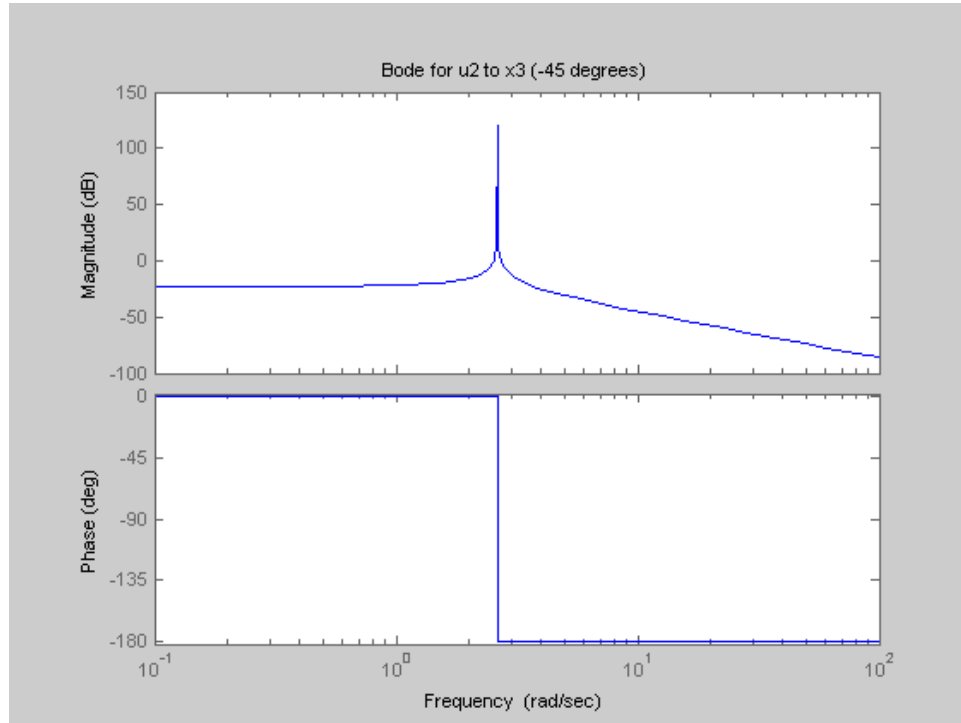


Figure 11: Bode plot for  $\frac{\Delta x_3(j\omega)}{\Delta u_2(j\omega)}$  for  $\Delta x_{3N} = -45^\circ$

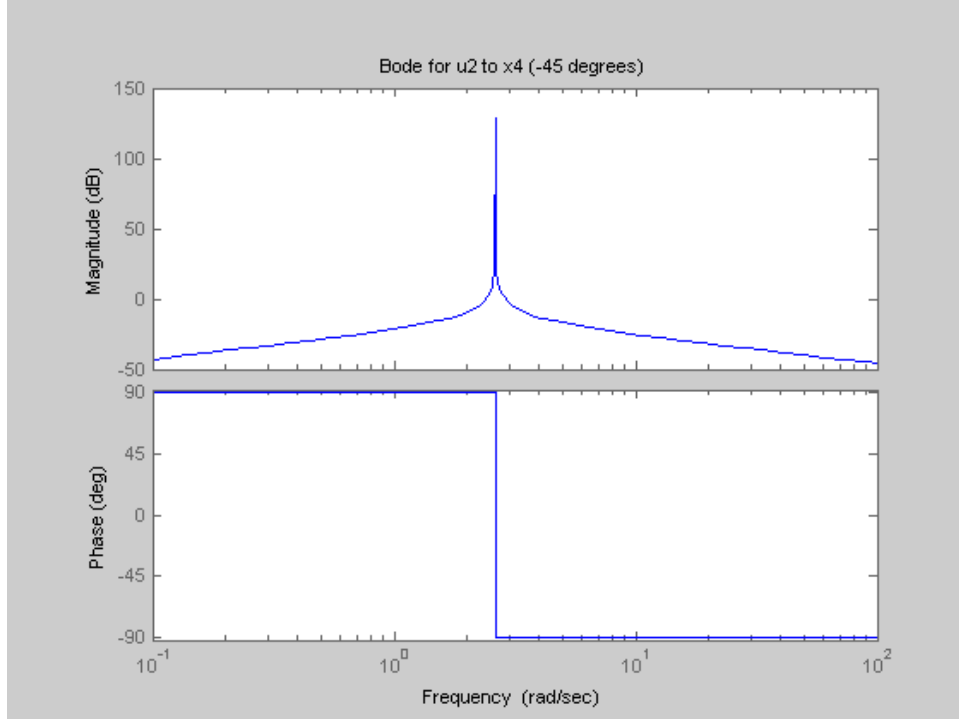


Figure 12: Bode plot for  $\frac{\Delta x_4(j\omega)}{\Delta u_2(j\omega)}$  for  $\Delta x_{3N} = -45^\circ$

### 3 Effects of Constant Angular Rate About Vertical Axis

We assume that  $\dot{\theta}_1 = x_{2N}$  takes on constant values between  $0^\circ/sec$  and  $720^\circ/sec$ . We wish to determine the effect of this nominal angular rate on the eigenvalues of  $\mathbf{F}$  under the three conditions previously explored.

Figures 13, 14, and 15 show plots of the real and imaginary part of the eigenvalues for each of the three cases explored as  $\dot{\theta}_1 = x_{2N}$  varies between  $0^\circ/sec$  and  $720^\circ/sec$ . The rotation of the upright introduces a centripetal force which changes the values of the first two eigenvalues, which control the dynamics of the transverse arm. We begin by investigating 13, showing the zero degree case. We see that the centripetal force introduces an oscillatory mode into the system, as evidenced by the pure imaginary eigenvalues that grow with the square root of the angular rate. This makes physical sense, as the centripetal force will act as a restoring moment towards the equilibrium point of  $\theta_2 = x_3 = 0^\circ$ . The force acts in the horizontal direction and its moment arm is proportional to  $\sin(\theta_2)$ , so we expect to see an oscillatory mode analogous to that of a simple pendulum.

In the  $\pm 45^\circ$  cases, we see similar effects. In both 14 and 15 we see that  $\dot{\theta}_1 \approx 400^\circ/sec$  appears to be a special point - in the  $45^\circ$  case, the eigenvalues switch from being entirely real to all zero to entirely imaginary at this point, and in the  $-45^\circ$  case the imaginary eigenvalues suddenly cross through zero. This angular velocity corresponds to the point at which the centripetal torque exactly balances the gravitational torque for the moment arm corresponding to  $\pm 45^\circ$ . For rotations slower than  $400^\circ/sec$ , gravitational effects dominate. In the  $45^\circ$  case, this means the system is unstable, for reasons discussed in the previous assignment - the torque required to balance gravity decreases

with increasing angle, so perturbations lead to unbounded growth. In the  $-45^\circ$  case, the system is stable and oscillatory, and becomes more oscillatory with increasing angular velocity because the centripetal force acts as an additional restoring torque. At  $400^\circ/sec$ , gravity and the centripetal force are perfectly balanced, so all eigenvalues are zero. For rotations faster than  $400^\circ/sec$ , the centripetal effects dominate. In the  $-45^\circ$  case, the system is still stable, and the oscillatory imaginary eigenvalues continue to increase with angular velocity at the same rate as before. For the  $45^\circ$  case however, the system dynamics have changed - the overall torque now acts as a restoring torque, and we have oscillatory imaginary eigenvalues.

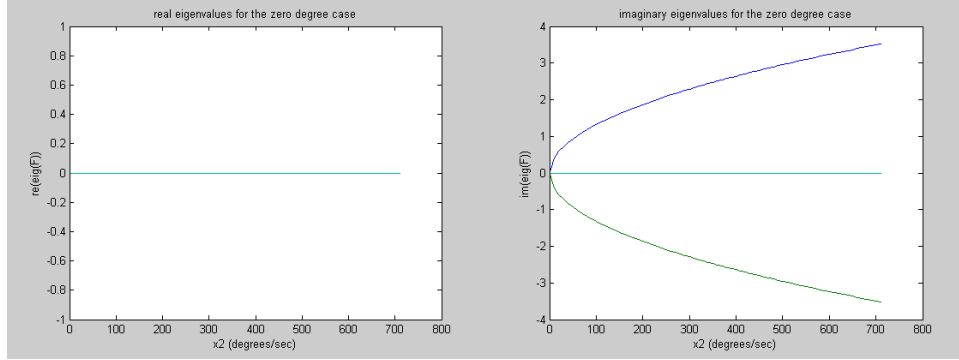


Figure 13: Plot of  $\text{im}(\text{eig}(\mathbf{F}))$  at  $x_{3_N} = 0^\circ$  as  $\dot{\theta}_1 = x_{2_N}$  varies between  $0^\circ/sec$  and  $720^\circ/sec$ .

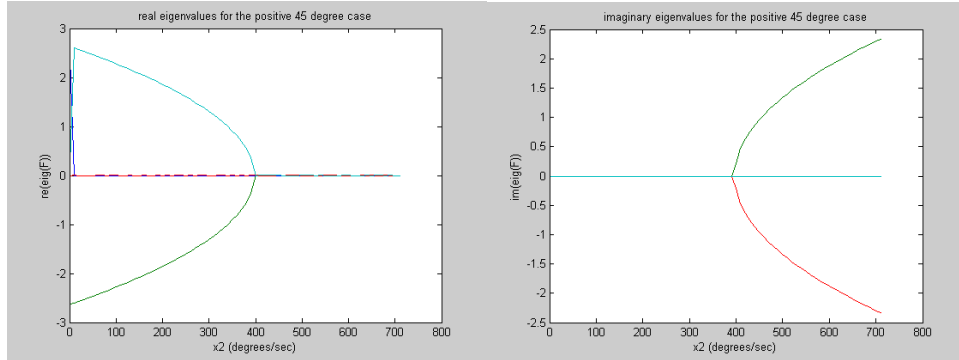


Figure 14: Plots of  $\text{eig}(\mathbf{F})$  at  $x_{3_N} = 45^\circ$  as  $\dot{\theta}_1 = x_{2_N}$  varies between  $0^\circ/sec$  and  $720^\circ/sec$ .

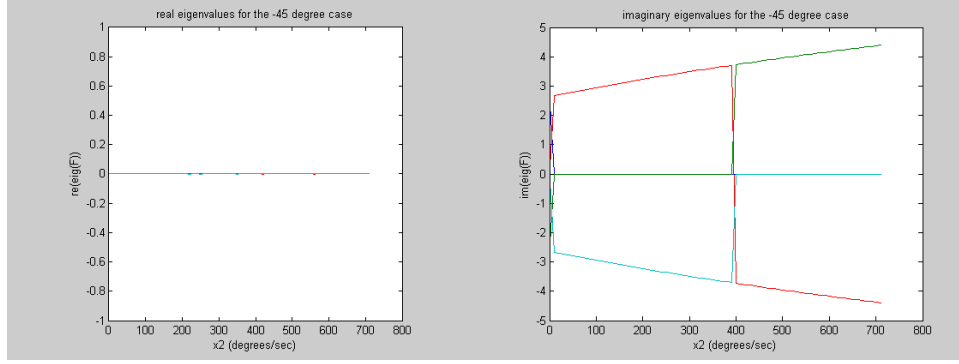


Figure 15: Plot of  $\text{im}(\text{eig}(\mathbf{F}))$  at  $x_{3_N} = -45^\circ$  as  $\dot{\theta}_1 = x_{2_N}$  varies between  $0^\circ/\text{sec}$  and  $720^\circ/\text{sec}$ .

## Conclusions

The results of these analyses show that important qualities of dynamic systems (such as stability to perturbation) can often be accurately determined through linearization about points of interest. Linearization can simplify the mathematics required to analyze a complicated nonlinear system a great deal, making it a very useful tool in the study of dynamic systems. It is important to note, however, that these results are valid *only in the vicinity of the linearization point*. For example, our linearized equations about  $\theta_{2_N} = -45^\circ$  indicate that  $\theta_2$  will increase linearly with increasing  $\dot{\theta}_1$  for arbitrarily large values of  $\dot{\theta}_1$ . Physically, this is quite incorrect -  $\theta_2$  may only increase until it reaches  $0^\circ$ . While linearization is a powerful tool, we must be careful to apply linearized equations only where they are valid.